Journal of Engineering and Technology for Industrial Applications

ISSN ONLINE: 2447-0228

ITEGAM-JETIA

Manaus, v.12 n.57, p. 888-895. January/February, 2026.

DOI: https://doi.org/10.5935/jetia. v12i57.3121

RESEARCH ARTICLE

OPEN ACCESS

EVALUATION OF THE PERFORMANCE OF COMPUTATIONAL MODELS FOR THE ANALYSIS OF THE PROTECTION OF MIRROR COATINGS WITH DATA OBTAINED USING ELECTROCHEMICAL IMPEDANCE SPECTROSCOPY

Juan Carlos Gonzalez-Islas[1], Ernesto Bolaños-Rodríguez *[2], Asdrúbal López-Chau[3], Gildardo Godínez-Garrido[4], Aldo Márquez- Grajales[5] and Fernando Salas-Martínez[6]

[1,4,5,6] Instituto de Ciencias Básicas e Ingeniería-Universidad Autónoma del Estado de Hidalgo. Pachuca-Tulancingo Km. 4.5, Carboneras, 42184, El Álamo, Mineral de la Reforma, Estado de Hidalgo, México.
[2] Escuela Superior de Tizayuca-Universidad Autónoma del Estado de Hidalgo. Carretera Federal Tizayuca-Pachuca Km 2.5. 43800. Tizayuca, Estado de Hidalgo, México.
[3]Centro Universitario UAEM Zumpango, Universidad Autónoma del Estado de México, 55600, México

[1]http://orcid.org/0000-0002-2190-0660, [2]http://orcid.org/0000-0002-1432-7720, [3]http://orcid.org/0000-0001-5254-0939
[4]https://orcid.org/0000-0002-7177-3815, [5]https://orcid.org/0000-0001-9567-2069, [6]https://orcid.org/0000-0002-5104-5167

Email: juan_gonzalez7024@uaeh.edu.mx, ebolanos@uaeh.edu.mx, gildardo.godinez@uaeh.edu.mx, aldo_marquez@uaeh.edu.mx, fernando_salas@uaeh.edu.mx, alchau@uaemex.mx

ARTICLE INFO

Article History
Received: December 12, 2025
Revised: January 10, 2026
Accepted: January 15, 2026
Published: February 28, 2026

Keywords:
Polynomial fit, Cubic Spline fitting, Local Regression Smoothing, Electrochemical Impedance Spectroscopy, Protective Coatings, Mirrors.

ABSTRACT

This research predicts the impedance function of mirror coatings using three curve fitting models implemented in MATLAB, such as: Polynomial fit (Polyfit), Cubic Spline fitting (CSAPS) and Local Regression Smoothing (LOESS) to carry out the analysis of the protection of mirror coatings in which the Electrochemical Impedance Spectroscopy (EIS) technique has been used. The electrochemical impedance parameters and their equivalent circuits have been measured from the data recorded at 5 and 24 hours of exposure of the sample under study to the aggressive agent sodium chloride at weight 3%. The methodology is structured into training (parameter calibration) and testing (performance evaluation) stages. The performance of the models in the training stage is carried out by cross-validation and in the testing stage it is quantified using the Root Mean Square Error (RMSE) and the determination coefficient (R^2). The main results obtained show that the CSAPS method at 5 and 24 hours after exposing the system to the electrolyte is the most robust and consistent in cross-validation and the most accurate and reliable in performance when evaluating the complete data set with an $RMSE(5hr) = 3.40$ and $RMSE(24hr) = 3.78$, and $R^2 \approx 1.0$ in both cases .

I. INTRODUCTION

Mirrors consist of a glass substrate onto which a layer of silver is deposited, followed by protective copper coatings and a paint scheme: primer and finish, which extend the product's useful life [1]. It is important to evaluate the performance of the protection provided by these coatings, and one of the techniques used for this purpose is EIS. The EIS technique is widely used for studies of electrochemical corrosion processes such as those occurring in nonconductive metal-coatings-electrolyte systems [2]. To use this technique, small perturbations are applied to the potential or current system and the response obtained is analyzed, the spectrum corresponding to the impedance of the system is represented and by means of the selected equivalent circuit, the values of the processes that have taken place due to the applied perturbation are extracted [3]. The study of systems using EIS is possible because of the direct relationship between the behavior of the real system and the theoretical electrical circuit constituted by a discrete set of resistors and capacitors called equivalent electrical circuit [4]. It is important to determine models that fit the impedance function curve based on the Nyquist diagram in EIS because these models allow for the physical interpretation of the experimental data obtained and the quantification of the electrochemical behavior of the system studied, as well as the evaluation of the degree of protection provided by the coatings.

Fitting models to the impedance curve of the Nyquist plot is essential because it transforms complex experimental data into interpretable physical parameters, allowing the behavior of electrochemical systems to be evaluated, compared, diagnosed, and predicted with high scientific rigor. That is why, the goal of this paper is to evaluate the performance of three models adjusted to the curve generated in the Nyquist diagram with real experimental data obtained by electrochemical impedance spectroscopy through the use of metrics in the calibration and testing stages in order to determine the best performance and simulate the protective behavior of mirror coatings in the presence of aggressive agents at 0, 5, and 24 hours of exposure. For which the following research question is formulated: Which of the three fitting methods Polyfit, CSAPS, and LOESS to the impedance function curve generated with data obtained with EIS performs best?

II. BACKGROUND

II.1 DESCRIPTION OF COATING BEHAVIOR USING EIS

These systems present different impedance spectra depending on the degree of deterioration of the paint film and the phenomena taking place at the metal-paint interface. The impedance spectra represented in the Nyquist diagram in the corrosion process will be briefly discussed with their theoretical interpretation [1]. Initially, when the paint film is intact: The behavior of the intact paint film is typically capacitive as it corresponds to a dielectric. The passage of electrolytes and other corrosive elements does not occur through the paint film because the resistance value of the film R_p is very high. When the paint film is in ideal condition, the Nyquist diagram takes the form of a straight line that forms a certain angle with the imaginary axis. In this case, the behavior is purely capacitive and is associated with a capacitor in parallel with a high ohmic resistance of the paint. The response in the Nyquist diagram is similar to a capacitor with phase angles close to 90° and very high values of the impedance modulus Penetration of aggressive agents through the paint: The access of the aggressive agents by the electrolyte through the film causes variation in the electrical parameters of the system. This shows that the film resistance R_p decreases and decreases, so that the line increases and decreases forming a semicircular arc in the Nyquist diagram Contact of the aggressive agent with the metal surface: As time passes, the electrolyte enters more easily because it has degraded the paint film and, consequently, the resistance R_p drops steadily.

This effect is evident in the impedance spectrum with a Nyquist diagram, where the semicircle has a smaller diameter. The equivalent circuit corresponding to the Nyquist diagram of the film of deteriorated paints offers a lower resistance to the electrolyte input, and consequently the value of R_t has dropped to values detected by the equipment. The prolongation of this arc on the abscissa axis gives the value of R_t at the time of measurement. As time goes by and the deterioration process of the paint progresses, the value of R_t decreases, consequently, the electrolyte ingress is more and more favored, and consequently, the value of C_d rises due to the contribution of the dielectric constant With formation of corrosion products: In these systems, corrosion can occur after long periods of exposure, with a new time constant at low frequencies, which is associated with the phenomena of metallic corrosion. The resistance value of the paint film to the passage of the electrolyte R_p is so small that the concentration of aggressive agents at the paint-metal interface is sufficient to initiate metallic corrosion processes. Metallic corrosion may be limited by the diffusion of matter through the paint film, as may be the case with oxygen diffusion, and then the impedance diagram at lower frequencies takes the form of a straight line at 45° to the abscissa axis.

II.2 ADJUSTMENT METHODS

Electrochemical Impedance Spectroscopy (EIS) is a fundamental technique for assessing the protective performance of mirror coatings, as it enables the characterization of resistive, capacitive and diffusion-related processes governing degradation. To enhance the interpretability of raw EIS data prior to equivalent-circuit modeling, smoothing and curve-fitting methods such as Polynomial Fitting (Polyfit), Cubic Smoothing Splines (CSAPS), and Local Regression Smoothing (LOESS) are increasingly used. Polyfit provides a simple parametric trend estimation that facilitates the identification of global impedance behavior; CSAPS offers flexible spline-based smoothing that preserves curvature and minimizes noise; while LOESS enables robust, local adaptation to spectral variations without imposing a global functional form. These methods improve denoising, reveal subtle frequency-dependent features, and support more reliable extraction of coating performance indicators [5], [6]. This study uses methods such as: Polyfit, CSAPS and LOESS because they are well suited to the actual characteristics of experimental impedance data, which tend to be nonlinear, noisy, and frequency-dependent [7].

II.2.1 Polynomial Fit (Polyfit)

Polynomial fitting seeks a polynomial $P_n(x)$ of degree n that minimizes the sum of squared errors (MSE) between the observed data y_i and the values predicted by the polynomial:

$$\hat{y} = P_n(x)$$

The prediction function is defined as equation 1:

$$\hat{y} = P_n(x) = \sum_{j=0}^{n} a_j x^j = a_0 + a_1 x + a_2 x^2 + \cdots + a_n x^n \quad (1)$$

Where a_j are the coefficients of the polynomial and n is the degree of the polynomial, which is the parameter to be optimized. The coefficients are determined by solving the system of least squares normal equations [8].

II.2.2 Cubic Spline Adjustment (CSAPS)

The CSAPS (Cubic Smoothing Spline) method produces a smoothing function that balances the fit to the data and the smoothness of the curve [9]. The function $y(x)$ is a cubic spline that minimizes the following objective function [10], equation 2:
$Minimizar$:

$$p \sum_{i=1}^{m} w_i \, (y_i - \hat{y}(x_i))^2 + (1-p) \int_{x_1}^{x_m} (\hat{y}''(x))^2 \, dx \tag{2}$$

Where:

- The first term is the weighted sum of the squared errors (lack of fit).
- The second term penalizes the curvature of the smoothness function $y(x)$.
- w_i are the weights (generally w_i = 1).
- p is the smoothing parameter ($0 \leq p \leq 1$), which is the key parameter to be optimized.
- If $p = 0$, a straight line is obtained by least squares (maximum smoothness).
- If $p = 1$, the cubic interpolating spline is obtained (minimum smoothness).

II.2.3 Local Regression Smoothing (LOESS)

LOESS (Locally Estimated Scatterplot Smoothing) is a nonparametric regression technique that fits low-degree regression models (usually linear or quadratic) to localized subsets of data [11]. To predict at point x, a local polynomial is fitted to the points within a neighborhood window, weighting points closer to x more heavily than those farther away [12]. The weighting $W(d)$ for a point x is based on the normalized distance d_i, equation 3:

$$d_i = \frac{|x - x_i|}{d_{max}} \tag{3}$$

Where:

d_{max} is the distance of the $k-th$ nearest neighbor to x.

III. MATERIALS AND METHODS

III.1 SAMPLE PREPARATION

A representative sample of the population of the technological process of mirror manufacturing is obtained by simple random sampling from the procedure given by Pérez [13], the same have the following characteristics: silver coating on the glass substrate, then protective deposits to the chemical copper silver and two coats of paints, a primary anticorrosive and a finishing coat. The average thicknesses of each are shown in Table 1.

Table 1: Average thickness of the glass, silver coating, opper coating and paint scheme (primary-finish) the specimens subjected to the experimental test using the Electrochemical Impedance Spectroscopy technique.

Glass thickness (mm) (mm)	Silver layer thickness (µm)	Copper layer thickness (µm)	Primary paint layer thickness (µm)	Finish paint layer thickness (µm)
3	0.07 ± 0.03	0.21 ± 0.04	30 ± 10	30 ± 10

Source: Authors, (2026).

III.2 DATA ACQUISITION

The electrochemical cell used in the EIS technique is shown in Figure 1. The working electrode, the test specimen, is fixed with screws between two plates. The upper plate has a hole with a surface area of 12.6 cm^2 through which the glass container is placed into which the electrolyte solution, sodium chloride (NaCl) is introduced at 3% by weight. The vessel consists of a central tube with a conical end, where the reference electrode (saturated calomel electrode) is located, and the auxiliary electrode is a large surface area graphite sheet that is placed around it.

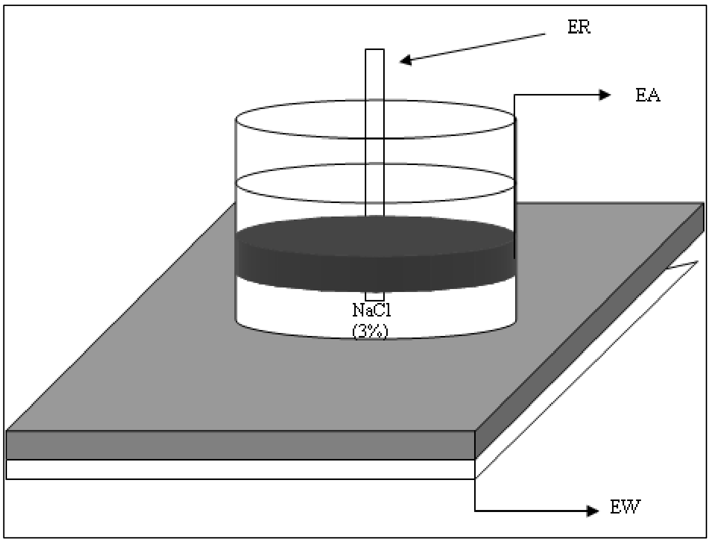

Figure 1: Electrochemical cell used in the impedance technique. Where EW: Working electrode, mirror specimen (Silver-Copper-Paint), EA: Auxiliary electrode, graphite sheet and ER: Reference electrode, saturated calomel electrode.
Source: Authors, (2026).

The electrolyte used is 3% sodium chloride, which has a $pH = 5.53$ and a conductivity of 75.8 mS/cm. Measurements of EIS were taken at 0, 5 and 24 hours (prolonged exposure) after the electrolyte was introduced into the measuring cell. The impedance measurements were performed with the use of a Solartron model 1286 potentiostat coupled to a frequency response analyzer of the same brand, model 1255, which also serves as a generator of alternating current (A.C.) signals. A Kemo filter (VBF8) is used to eliminate the noise in the signal and the visual control of the signals entering the analyzer is performed by means of an oscilloscope. The electrochemical cell is placed in a Faraday box to minimize noise from external sources. The amplitude of the applied signal is 10 mV and it has been worked in a frequency domain from 100 kHz to 1 mHz.

III.3 FITTING METHODOLOGY FOR THE IMPEDANCE FUNCTION

The prediction of the impedance function Z(w) of mirror coatings is addressed using three curve fitting techniques implemented in MATLAB: CSAPS, and LOESS. The methodology is structured into training (parameter calibration) and testing (performance evaluation) stages.

III.3.1 Training

The objective of the parameter training and calibration stage is to determine the optimal parameters for each model (degree n for Polyfit, parameter p for CSAPS, and span α for LOESS) that offer the best compromise between fit and generalization. Then, the k-fold cross-validation method with $k = 10$ is used to estimate the performance of the models in the data population. The data is randomly assigned to the k subsets (folds) to ensure that each fold represents the total variability of the data [14]. Parameter optimization: Within each iteration, a range of values for each parameter of the models is evaluated. The average performance across the 10 folds is used to select the final parameter value that minimizes the error.

III.3.2 Testing

Once the optimal parameters have been selected, the final evaluation of the performance of the models is carried out over the total data set.

III.4 PERFORMANCE METRICS

The performance of the models in the training (cross-validation) and testing stages is quantified using the Root Mean Square Error (RMSE) and the Coefficient of Determination (R^2) [15].

III.4.1 Root Mean Square Error (RMSE)

RMSE measures the average magnitude of errors. It is the square root of the mean of the squared errors, expressed in the same units as the response variable [16]. A lower value indicates a better fit, equation 4.

$$RMSE = \sqrt{\frac{1}{m}\sum_{i=1}^{m}(y_i - \hat{y}_i)^2} \qquad (4)$$

III.4.2 Coefficient of Determination (R^2)

R^2 represents the proportion of variance in the dependent variable that is predictable from the independent variables [17]. A value closer to 1 indicates that the model explains a greater proportion of the variability in the data, see equation 5.

$$R^2 = 1 - \frac{\sum_{i=1}^{m}(y_i-\hat{y}_i)^2}{\sum_{i=1}^{m}(y_i-\bar{y})^2} \quad (5)$$

Where y_i is the observed value, $\hat{y}$ is the predicted value, $\bar{Y}$ is the mean of the observed values.

IV. ANALYSIS AND DISCUSSION OF RESULTS

The analysis is based on the evaluation of the performance of three curve fitting methods implemented in MATLAB (Polyfit, CSAPS and LOESS) to predict the impedance function $Z(w)$ of the coating after 5 and 24 hours of exposure to the aggressive agent. The evaluation focuses on the optimization stage (10-fold cross validation), the final performance with the optimal parameters, and the visual fit to the impedance curves (real part, imaginary part, and Nyquist diagram).

IV.1 ANALYSIS AND DISCUSSION OF RESULTS FOR PREDICTING IMPEDANCE FUNCTION FOR 5 HOURS

Table 2 shows the performance of the models when finding their best parameter (degree, p, or span) within the complete or validation dataset for 5 hours of exposure to the aggressive agent in the system.

Table 2: Parameters and metrics (best) for the three adjustment methods applied for t = 5 hours.

Method	Optimal Parameter	RMSE	R^2
Polyfit	Degree 15	82350.27	0.9958
CSAPS	p = 0.001	65732.04	0.9971
LOESS	span= 0.05	50479.49	0.9983

Source: Authors, (2026).

Accuracy (RMSE and R^2): The LOESS method with a span of 0.05, which implies very local smoothing, achieves a lower RMSE and the highest R^2, indicating that at the optimum point of its parameters, LOESS offers the most accurate fit to the impedance function. The Polyfit and CSAPS fits also perform well (R^2 > 0.99), although with slightly higher errors. Parameter implications: Polyfit (Degree 15) is necessary to capture the complex shape of the impedance data (especially the imaginary part), but this introduces a risk of overfitting. CSAPS (p = 0.001), such a low smoothing parameter, close to 0, indicates that the adjustment strongly prioritized smoothness over exact data fidelity. LOESS (span=0.05): An extremely low span (5% of the data) confirms that to achieve the best accuracy, LOESS had to perform very localized regression adjustments, minimizing the global smoothing effect and closely following data fluctuations. Table 3 shows the critical metric for evaluating the robustness and generalization capacity of the model, as it uses data not seen in each iteration.

Table 3: Robustness and generalization capacity of the model for the three fitting methods applied for t = 5 hours.

Method	$RMSE_{mean}$	$RMSE_{SD}$	R^2_{mean}	
Polyfit	270056.49	262349.2	0.9120	0.1568
CSAPS	65733.61	0.6950	0.9971	≈ 0.0000
LOESS	93188.91	55912.77	0.9917	0.0110

Source: Authors, (2026).

SAPS is the most robust and consistent model, as shown by its standard deviation (SD) metrics, implying that the accuracy of CSPAS does not vary significantly when changing the training/validation dataset. This is evidence that the model has not overfitted the training set. R^2_SD = 0.0000 confirms perfect consistency. For Polyfit, there is evidence of overfitting due to the very high values of average RMSE and standard deviation. The 15th degree model fits too closely to the specific noise of the training set, failing to generalize to the validation data. LOESS shows good performance results but is less consistent. The R^2_{mean} is high, demonstrating its good generalization capacity. However, its $RMSE_{SD}$ is significantly higher than that of CSAPS, indicating moderate sensitivity to data partitioning and making it less consistent. Table 4 shows the results for the complete dataset (Test).

Table 4: Metrics for the three adjustment methods applied for t = 5 hours.

Method	RMSE	R^2
Polyfit	75791.97	0.9974
CSAPS	3.9242	≈1.0000
LOESS	31553.62	0.9996

Source: Authors, (2026).

The final metrics in the full dataset confirm the superiority of CSAPS in terms of robustness, as it has very low RMSE values and a perfect R^2. The consistency of CSAPS translates into an adjustment capacity that surpasses the other two methods. Its mechanism that prioritizes smoothing (p = 0.001) managed to capture the actual impedance function in an effective and robust manner. LOESS maintains its high performance with an RMSE of 31.553 and an R^2 of 0.9996, making it the second-best method. Polyfit has a high R^2 of 0.9974, although it has the highest error of the three methods, confirming that although it can plot the general trend, its fit is less accurate. Figure 2 shows the fit of the three methods on the real and complex impedance data.

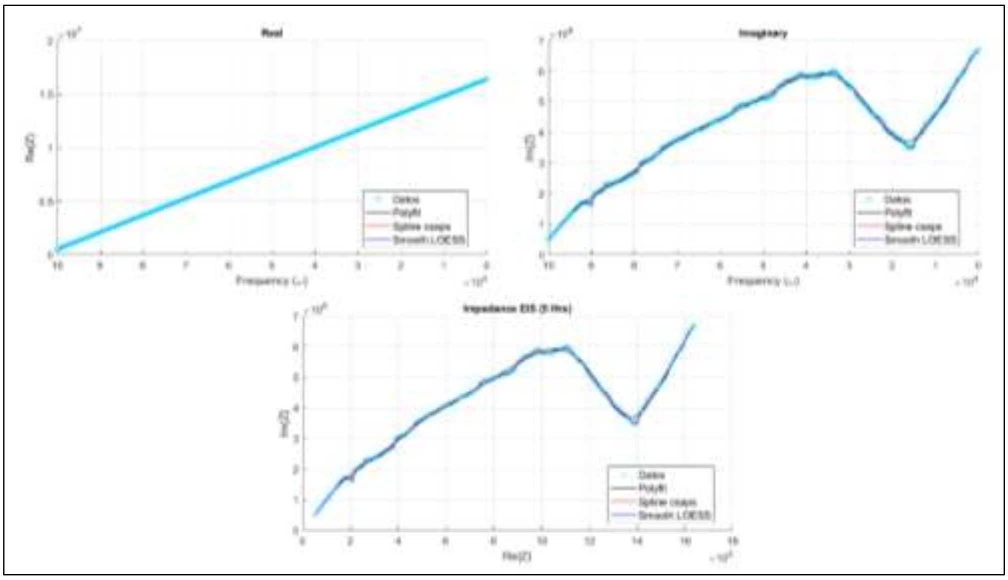

Figure 2: Adjustment of the three methods on real and imaginary impedance data for t = 5 hours.
Source: Authors, (2026).

The real part of the impedance has an almost linear trend with frequency, which means it can be adjusted. Visually, the three methods overlap almost perfectly on the data, which is consistent with the high R^2 values of all models. The imaginary component has a more complex shape with a curvilinear variation and possibly multiple time constants. Both CSAPS and LOESS follow the fluctuations in the data with great fidelity. Polyfit also fits well, but LOESS better captures the changes in curvature observed in the mid frequencies. The Nyquist diagram is the representation most sensitive to the adjustment of the equivalent circuit parameters. The diagram for 5 hours of exposure shows a depressed semicircle, indicating the presence of a constant phase element due to relaxation dispersion in the coating/interface. The overlapping curves show that CSAPS and LOESS offer the smoothest predictions and best fit the pattern of the depressed semicircle, especially at the vertex and in the low-frequency region. Graphically, the large differences in RMSE seen in the tabular results are not apparent, underscoring the importance of numerical metrics (RMSE) for discriminating between visually similar fits.

IV.2 ANALYSIS AND DISCUSSION OF RESULTS FOR PREDICTING IMPEDANCE FUNCTION FOR 24 HOURS

This section analyzes the performance of the three fitting methods (Polyfit, CSPAS, and LOESS) for predicting the impedance function Z(w) of the coating during 24 hours of exposure to the aggressive agent in the system. Table 5 shows the optimal performance achieved by each model when selecting its best parameter (degree, p, or span) in the training (validation) dataset.

Table 5: Parameters and metrics (best) for the three adjustment methods applied for t = 24 hours.

Method	Optimal Parameter	RMSE	R^2
Polyfit	Degree 14	149070.7	0.9807
CSAPS	p = 0.01	177630.8	0.9408
LOESS	span = 0.05	97418.67	0.9905

Source: Authors, (2026).

As at 5 hours, LOESS with a span of 0.05, very local smoothing, achieves the lowest RMSE and the highest R^2. This confirms that LOESS is the method capable of achieving the most accurate fit to the data in its optimal configuration. By prioritizing smoothness (p = 0.001), CSAPS obtains a significantly lower R^2 (0.9408) and a higher RMSE than the other two methods at this stage. This suggests that at 24 hours, the impedance function presents more noise or fluctuations than CSAPS, due to its extreme penalty on curvature, is unable to capture efficiently. Polyfit with grade 14 shows a good R^2 (0.9807), outperforming CSAPS in direct fit. The 10-fold cross-validation evaluation is essential for determining how well the model generalizes to unseen data and how consistent its performance is (low standard deviation), see Table 6.

Table 6: Robustness and generalization capacity of the model for the three fitting methods applied for t = 24 hours.

Method	$RMSE_{mean}$	$RMSE_{SD}$	R^2_{mean}	R^2_{SD}
Polyfit	377985.63	286554.5	0.8124	0.3038
CSAPS	177638.49	3.4020	0.9408	≈0.0000
LOESS	170240.04	88776.41	0.9701	0.0295

Source: Authors, (2026).

The CSAPS model is once again the most robust and consistent with the 24-hour dataset. Its R^2 is 0.0000 and its $RMSE_{SD}$ is only 3.4020. This indicates that although its average accuracy is not the highest (R^2_{mean} = 0.9408), its performance is consistent across different random partitions of the data, which is a critical feature against overfitting.

LOESS achieves the best average R^2 and the lowest average RMSE in cross-validation. This suggests that, on average, it is the method that best generalizes the shape of the impedance, although its high $RMSE_{SD}$ makes it less consistent than CSAPS. Polyfit, with its high degree, 14, exhibits overfitting behavior than at 5 hours. The average RMSE and high standard deviation reveal that the fit is extremely sensitive to data selection, resulting in the worst generalization performance R^2 mean. Table 7 shows the results for the entire dataset (test).

Table 7: Metrics for the three adjustment methods applied for t = 24 hours.

Method	RMSE	R^2
Polyfit	134820.0	0.9876
CSAPS	5.7802	1.0000
LOESS	47469.40	0.9985

Source: Authors, (2026).

The consistency of CSAPS observed in cross-validation is confirmed by an almost perfect fit in the complete dataset of RMSE and $R^2 \approx 1.00$. Although the curvature penalty mechanism initially limited its R^2 in the benchmark, it proves to be the most effective strategy for a precise and robust final fit. Figure 3 shows the fit of the three methods to the impedance data at 24 hours of exposure.

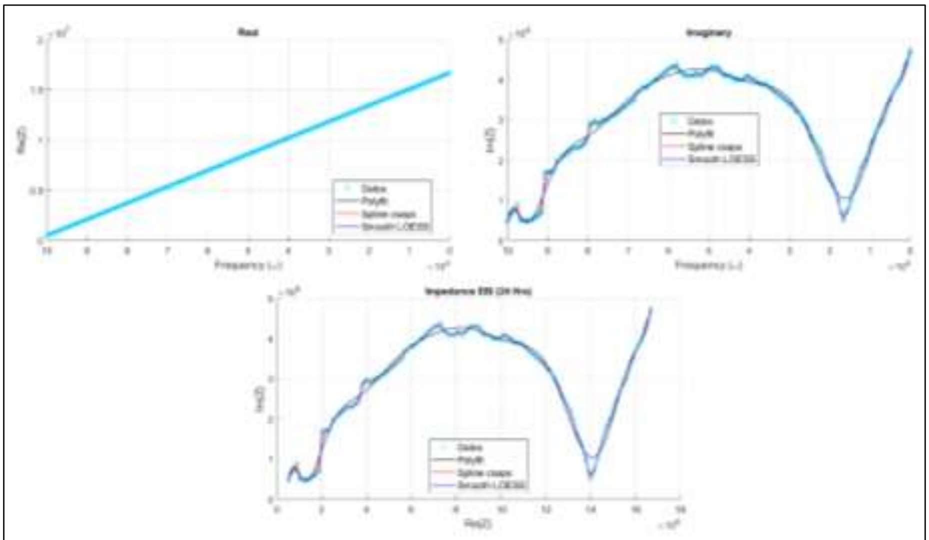

Figure 3: Adjustment of the three methods on real and imaginary impedance data for t = 24 hours.
Source: Authors, (2026).

As at 5 hours, the real part shows a simple trend. The three methods overlap on the data, which is consistent with the high final R^2 values. The imaginary part shows a smoother curve than at 5 hours, with a more defined plateau region between frequencies 7.10^4 Hz and 5.10^4 Hz. All methods follow the trend very well. CSAPS and LOESS fit the slight curvature and detail in the high-frequency flank most accurately. Polyfit follows the trend but may exhibit subtle oscillations inherent in high-degree polynomials. The 24-hour Nyquist diagram shows two distinct arcs, a depressed high-frequency arc and the beginning of a second very low-frequency arc. This is typical of behavior where ion diffusion has already been activated. The CSAPS and LOESS curves trace the pattern of the two arcs with great fidelity and smoothness. The near-perfect fit of the CSAPS suggests that its fitting function passes exactly through the data points, which is visually indistinguishable from the LOESS fit.

V. CONCLUSIONS

The CSAPS method is identified as the most suitable prediction model for the impedance function after 5 hours of exposure, although LOESS achieved the best fit in the benchmark evaluation. CSAPS demonstrated superior robustness and consistency in cross-validation ($RMSE_{SD} \approx 0$), resulting in the most accurate and reliable performance when evaluating the entire data set ($R^2 = 1.00$). The Polyfit method is ruled out as a primary option due to its strong tendency to overfit, evidenced by the high variation in cross-validation performance. For predicting impedance function at 24 hours, the CSAPS method, with its extreme penalty for curvature (p = 0.001), is the predictor of choice due to its excellent performance. Although LOESS demonstrated the highest accuracy in pointwise fitting and the best average generalization ability in cross-validation, the unmatched robustness of ($RMSE_{SD} \approx 3$ and $R^2\_SD \approx 0.00$) led to an almost perfect final fit to the test set ($R^2 \approx 1.00$). This result is fundamental in a scientific context, as it prioritizes reliable and consistent performance across different data subsets. The Polyfit method is excluded because of high variability and the risk of overfitting. Future work will focus on evaluating the proposed modeling strategies across a wider range of EIS datasets, including additional exposure times and coating systems, to assess their robustness under varying degradation mechanisms. Further refinement of the CSAPS and LOESS approaches such as adaptive smoothing parameters or hybrid integration with equivalent-circuit models may improve predictive accuracy and physical interpretability. Additionally, extending the analysis to larger datasets will enable more rigorous statistical validation and strengthen the generalization capability of the models.

VI. AUTHOR'S CONTRIBUTION

Conceptualization: Ernesto Bolaños-Rodríguez, Juan Carlos González-Islas.
Methodology: Juan Carlos González-Islas, Asdrúbal López-Chau, Gildardo Godínez-Garrido and Aldo Márquez-Grajales.
Investigation: Ernesto Bolaños-Rodríguez, Asdrúbal López-Chau, Aldo Márquez-Grajales and Fernando Salas Martínez.
Discussion of results: Ernesto Bolaños-Rodríguez, Juan Carlos González-Islas, Asdrúbal López-Chau, Gildardo Godínez-Garrido and Aldo Marquez-Grajales
Writing – Original Draft: Ernesto Bolaños-Rodríguez, Juan Carlos González-Islas and Fernando Salas Martínez
Writing – Review and Editing: Ernesto Bolaños-Rodríguez, Juan Carlos González-Islas, Asdrúbal López-Chau, Gildardo Godínez-Garrido, Aldo Marquez-Grajales and Fernando Salas Martinez
Supervision: Ernesto Bolaños-Rodríguez, Juan Carlos González-Islas.
Approval of the final text: Ernesto Bolaños-Rodríguez, Juan Carlos González-Islas, Asdrúbal López- Chau, Gildardo Godínez-Garrido, Aldo Marquez-Grajales and Fernando Salas Martinez.

VII. ACKNOWLEDGMENTS

We would like to thank our colleagues at the Corrosion Laboratory of the Chemical Engineering Department at the School of Industrial and Mining Engineering at the University of Vigo in Galicia, Spain, for their valuable collaboration in conducting the experimental tests using the electrochemical impedance spectroscopy technique.

VIII. REFERENCES

[1] E. Bolaños-Rodríguez, S. Gil-Fundora, and W. Francisco-Martín, "Determination of the protection behavior of coatings on mirrors using the Electrochemical Impedance Spectroscopy technique," *Journal of Metallurgy*, vol. 39, no. 3, pp. 210–214, 2003, doi: 10.3989/revmetlm.2003.v39.13.331.

[2] I. Obot and I. Onyeachu, "Electrochemical frequency modulation (EFM) technique: Theory and recent practical applications in corrosion research," *Journal of Molecular Liquids*, vol. 249, pp. 83–96, 2018, doi: 10.1016/molliq.2017.11.006.

[3] B. Ramírez Barat and E. Cano Díaz, "In situ evaluation of protective coatings for metallic cultural heritage using electrochemical impedance spectroscopy," *Ge-Conservation*, vol. 8, pp. 6–13, 2015, doi: 10.37558/gec.v8110.278.

[4] S. Papavinasam, R. Rebok, L. Yeng, and N. Berki, *Advances in Electrochemical Techniques for Corrosion Monitoring and Laboratory Corrosion Measurements*. West Conshohocken, PA, USA: ASTM International, 2019, doi: 10.1050/STP1506

[5] A. Cristoforetti, S. Rossi, F. Deflorian, and M. Fedel, "On the Limits of the EIS Low-Frequency Impedance Modulus as a Tool to Describe the Protection Properties of Organic Coatings Exposed to Accelerated Aging Tests," Coatings, vol. 13, no. 3, pp. 598, Mar. 2023, doi: 10.3390/coatings13030598.

[6] X. Liu, W. Li, and Y. Song, "Electrochemical Impedance Spectroscopy Analysis of Coating Degradation Using Advanced Data-Smoothing and Curve-Fitting Approaches," Electrochim. Acta, vol. 389, pp. 138–149, Jan. 2021, doi: 10.1016/j.electacta.2021.138149.

[7] B. Py, "Gaussian-processes for the analysis of electrochemical-impedance spectroscopy data: prediction, filtering, and active learning," ChemRxiv, 2022, doi: 10.26434/chemrxiv-2022-rs2m8

[8] S. Zhao, Y. Jiang, W.-P. He, et al., "Detrended fluctuation analysis based on best-fit polynomial," Frontiers in Environmental Science, vol. 10, art. 1054689, Nov. 2022, doi:10.3389/fenvs.2022.1054689

[9] A. Araveeporn, "The Estimating Parameter and Number of Knots for Nonparametric Regression Methods in Modelling Time Series Data," Modelling, vol. 5, no. 4, pp. 1413–1434, 2024, doi: 10.3390/modelling5040073

[10] S. O. Adams and O. J. Asemota, "The Efficiency of the Proposed Smoothing Method over the Classical Cubic Smoothing Spline Regression Model with Autocorrelated Residual," Journal of Mathematics and Statistics Studies, vol. 4, no. 1, pp. 26–40, 2023, doi: 0.31586/jml.2023.618

[11] M.-H. Chang, Y.-C. Huang, Y.-H. Cheng, C.-T. Terng, J. Chen y J. C. Jan, "Revisiting regression methods for estimating long-term trends in sea surface temperature," Nat. Hazards Earth Syst. Sci., vol. 24, pp. 2481–2494, 2024, doi:10.5194/nhess-2023-218

[12] L. H. Kushi, A. Zimbalist, K. H. Radimer, I. J. Ergas, J. M. Roh, C. P. Quesenberry y M. L. Kwan, "Utilization of locally estimated scatterplot smoothing (LOESS) regression to estimate missing weights in a longitudinal cohort of breast cancer patients," Ann. Epidemiol., vol. 104, pp. 55–60, 2025, doi: 10.1016/j.annepidem.2025.02.013

[13] C. Pérez, *Statistical Sampling Techniques*. Madrid, Spain: Garceta Grupo Empresarial, 2019.

[14] T. M. Dutschmann, L. Kinzel, A. ter Laak et al., "Large-scale evaluation of k-fold cross-validation ensembles for uncertainty estimation," J. Cheminformatics, vol. 15, art. 49, 2023, doi: 10.1186/s13321-023-00709-9

[15] D. Chicco and G. Jurman, "The coefficient of determination R-squared is more informative than SMAPE, MAE, MAPE, MSE and RMSE in regression analysis evaluation," PeerJ Comput. Sci., vol. 7, e623, Jul. 2021, doi: 10.7717/peerj-cs.623.

[16] T. O. Hodson, "Root-mean-square error (RMSE) or mean absolute error (MAE): when to use them or not," Geosci. Model Dev., vol. 15, no. 14, pp. 5481–5487, 2022, doi: 10.5194/gmd-15-5481-2022

[17] K. Li, "Informativeness of Performance Measures: Coefficients or R-Squareds?", J. Risk Financial Manag., vol. 17, no. 11, art. 481, Oct. 2024, doi: 10.3390/jrfm17110481